Original Article

Author for correspondence:
Masanobu Yamamoto,
Email: myama@ees.hokudai.ac.jp

CAMBRIDGE
UNIVERSITY PRESS

Late Miocene changes in C_3, C_4 and aquatic plant vegetation in the Indus River basin: evidence from leaf wax $\delta^{13}C$ from Indus Fan sediments

Kenta Suzuki[1], Masanobu Yamamoto[1,2] and Osamu Seki[1,3]

[1]Graduate School of Environmental Science, Hokkaido University, Kita-10, Nishi-5, Kita-ku, Sapporo 060-0810, Japan; [2]Faculty of Environmental Earth Science, Hokkaido University, Kita-10, Nishi-5, Kita-ku, Sapporo 060-0810, Japan and [3]Institute of Low Temperature Science, Hokkaido University, Kita-19, Nishi-8, Kita-ku, Sapporo 060-0810, Japan

Abstract

Vegetation changes in the Indus River basin within the past 10.8 million years were investigated based on the analysis of n-fatty acids and their carbon isotopes in sediments from IODP Site U1457 in the Laxmi Basin of the Arabian Sea. The $\delta^{13}C$ of long-chain n-C_{32} fatty acid shifted from −34 to −22 ‰ from 10 to 6.3 Ma, while the $\delta^{13}C$ of mid-chain n-C_{24} fatty acid was nearly constant at around −23 to −22 ‰ over the same period. This large difference in the $\delta^{13}C$ values suggests that the mid-chain fatty acids reflect the contribution of aquatic vascular C_3 plants. Before 6.3 Ma, the average chain length of n-fatty acids and the $\delta^{13}C$ values of long-chain fatty acids were negatively correlated, suggesting that the $\delta^{13}C$ values reflected the relative abundance of terrestrial C_3 versus aquatic C_3 plants in the Indus River basin and western India. After 5.8 Ma, the average chain length was variable, but the $\delta^{13}C$ values remained nearly the same, suggesting that the $\delta^{13}C$ values reflected heavier $\delta^{13}C$ values of both aquatic C_3 and C_4 plants. A three-end-member model calculation suggests that terrestrial C_3 plants were replaced by C_4 plants in the Indus River basin and western India from 9.7 or 8.2 to 6.3 Ma. Aridification in those areas during the late Miocene period may have driven the replacement of terrestrial C_3 plants by C_4 plants. An episodic increase in the abundance of terrestrial plants around 8 Ma is attributed to elevated precipitation by regionally enhanced moisture transport.

1. Introduction

The late Miocene period is notable for the occurrence of global cooling and the establishment of modern ecosystems (Herbert *et al.* 2016). Globally, there was a remarkable expansion of C_4 plants after 8 Ma (Cerling *et al.* 1998), and the drivers of this expansion remain uncertain (Edwards *et al.* 2010). C_4 plant species compose only 3 % of vascular plant species (Sage, 2004), but account for ~25 % of terrestrial photosynthesis (Still *et al.* 2003). C_4 plants dominate tropical and subtropical grasslands and savannas. They thrive in areas with high temperature, high aridity and low partial pressure of atmospheric carbon dioxide (pCO_2). Because C_3 and C_4 plants have different $\delta^{13}C$ values as a result of having different photosynthetic pathways, their relative abundances can be estimated geochemically by the analysis of leaf wax $\delta^{13}C$ in sediments (Chikaraishi *et al.* 2004). The late Miocene expansion of C_4 plants is thought to have taken place in low-pCO_2 environments (Cerling *et al.* 1998), but its triggers are disputed. However, both alkenone $\delta^{13}C$ and foraminifera $\delta^{11}B$-based pCO_2 reconstructions showed no evidence for a significant drop in pCO_2 during the late Miocene period (Pagani *et al.* 1999; Sosdian *et al.* 2018). Huang *et al.* (2007) reported positive shifts in leaf wax $\delta^{13}C$ and δD in sediments at ODP Site 722 in the Arabian Sea from 11 to 6.3 Ma, and suggested that aridification drove the expansion of C_4 plants in the Himalayan foreland and Arabian Peninsula. Tipple & Pagani (2007) concluded that the timing of geographical expansion of C_4 plants was not globally synchronous, and thus pointed towards more regional controls such as aridity, rainfall seasonality, growth season temperature, fire disturbance, etc., on the development of C_4-dominated ecosystems. On the other hand, Herbert *et al.* (2016) suggested that the pCO_2 decrease at 8 Ma, which was not shown by any pCO_2 proxy records but was assumed from the global cooling trend, triggered the expansion of C_4 plants. Polissar *et al.* (2019) recently reported evidence of synchronous expansion of C_4-dominated ecosystems across northwestern and East Africa after 10 Ma, which was not accompanied by aridification, and suggested that the decline of pCO_2 was a direct cause of C_4 grassland expansion.

In the present study, we analysed the $\delta^{13}C$ values of long- and mid-chain n-fatty acids derived from vascular plant leaf wax in sediments from the International Ocean Discovery Program
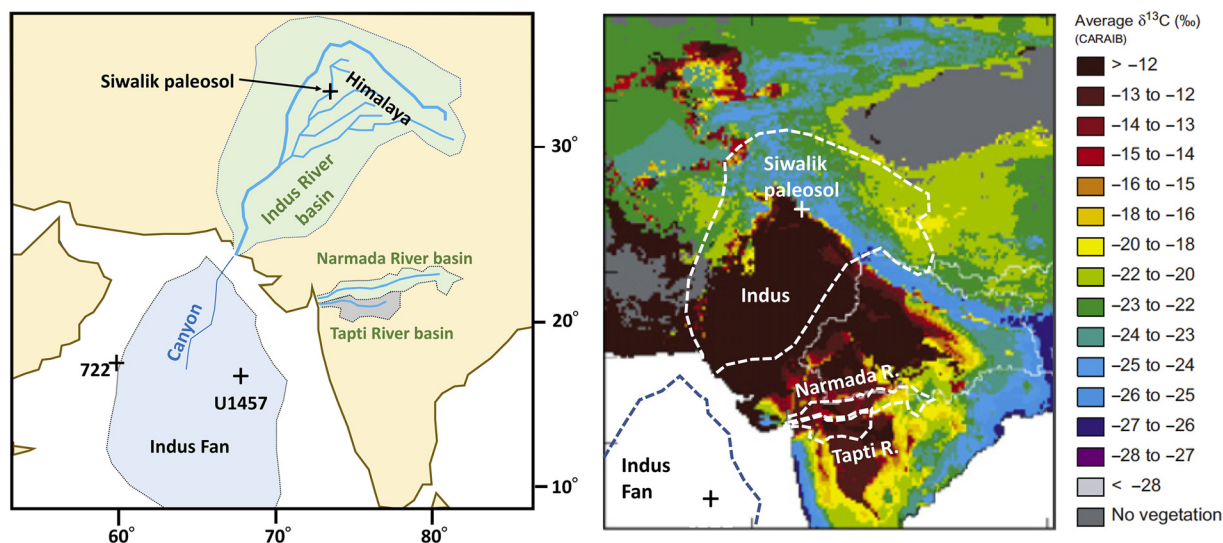
Fig. 1. Map showing the location of IODP Site U1457 and the average δ^{13}C of organic matter calculated by the CARAIB dynamic vegetation model for the present (Galy *et al.* 2008). Locations of ODP Site 722 and Siwalik palaeosol sequences are also indicated.

(IODP) Site U1457 in the Indus Fan of the Arabian Sea to characterize the development of C_3 and C_4 vegetation since 10.6 Ma. Because the sediments at the study site were delivered mainly from the Indus River basin and also possibly from western India (Pandey *et al.* 2016), the fatty acid results reflect vegetation changes in these areas.

2. Materials and methods

2.a. Samples

IODP Site U1457 was drilled in the Laxmi Basin (17° 09.95′ N, 67° 55.80′ E) at a water depth of 3534 m in the Arabian Sea (Fig. 1; Pandey *et al.* 2016). Site U1457 lies offshore of the western margin of India in the Arabian Sea, ~491 km from the Indian coast and ~750 km from the modern mouth of the Indus River, which is presumed to be the primary source of sediment to the area, at least during the Neogene Period (Pandey *et al.* 2016). Site U1457 is situated on the western edge of the Laxmi Basin, at the toe of the slope leading up to the structural and topographic high of the Laxmi Ridge.

Five lithological units were defined at Site U1457 (Fig. 2; Pandey *et al.* 2016). Unit I consists of a ~74 m thick sequence of Pleistocene nannofossil ooze and nannofossil-rich clay. Unit II is ~194 m thick and is dated to the early Pleistocene. It consists mainly of silty clay and sandy silt interbedded with very thin sandy silt turbidites. Unit III is ~450 m thick and consists of upper Miocene to lower Pleistocene silty claystone, silty sandstone, nannofossil chalk and nannofossil-rich claystone. Unit IV is ~227 m thick and consists of a mixture of interbedded lithologies dominated by claystone at the top of the unit and calcarenite, calcilutite, breccia and limestone towards the base of the unit. This unit is dated to the late Miocene. Lower Paleocene Unit V is ~30 m thick and mostly consists of claystone and volcaniclastic sediment. These sedimentary rocks directly overlie the basaltic basement.

The Indus Fan acquires most of its sediment load from the high-relief topography of the western Tibetan Plateau, Karakoram and Himalaya (Clift *et al.* 2004; Garzanti *et al.* 2005). In the sediments deposited at Site U457 during the last 600 ka, the ^{87}Sr/^{86}Sr and clay mineral ratios suggest the mixing of sediments derived from the

Indus River and Deccan Plateau (Yu *et al.* 2019). In comparison, the low ^{87}Sr/^{86}Sr and high ϵNd values in Site U1457 sediments older than 600 ka changed gradually into the high ^{87}Sr/^{86}Sr and low ϵNd values typical of the Himalayas, suggesting that the sediments were consistently derived from the Indus River before 600 ka, but the changes in the ^{87}Sr/^{86}Sr and low ϵNd values reflect the exposure of rock caused by the uplift of the Himalayas (Clift *et al.* 2019).

In the modern condition, the proportions of C_4 plants in the watersheds of the Indus and western Indian rivers, including the Narmada and Tapti rivers, are similarly high, whereas C_3 plants are more abundant in the upstream areas of the Indus River and the coastal areas of southwestern Peninsular India south of 2° N (Fig. 1; Galy *et al.* 2008). This distribution of C_4 plants suggests that the δ^{13}C of long-chain n-fatty acids was potentially affected by environmental changes in sediment source areas as well as changes in the main source areas of sediments.

A total of 75 samples were collected mainly from hemipelagic layers from a composite section between 1 and 990 m CSF-A (Units I to IV) at Site U1457. Cores and samples were stored at ~4°C until analysis. Samples were freeze-dried and pulverized.

2.b. Age–depth model

The succession of calcareous nannofossil and planktonic foraminifer events indicates that Site U1457 spans the early Paleocene through recent, albeit with a very long hiatus (~50 Myr) between lower Paleocene and upper Miocene sediments (Fig. 2). There are three other hiatuses around 8 Ma (~0.3 Myr), 6–4 Ma (~1.5 Myr) and 2 Ma (~0.2 Myr). The age–depth model was made based on nannofossil datums listed in Table 1.

2.c. Fatty acid δ^{13}C analysis

Lipids were extracted (× 3) from *c*. 3 g of dried sediment using a DIONEX Accelerated Solvent Extractor ASE-200 at 100°C and 1000 psi for 10 minutes with 11 ml of dichloromethane–methanol (6:4) and then concentrated. The extract was separated into two fractions with column chromatography (aminopropyl silica gel, i.d., 5.5 mm; length, 45 mm): 3 ml dichloromethane–2-propanol
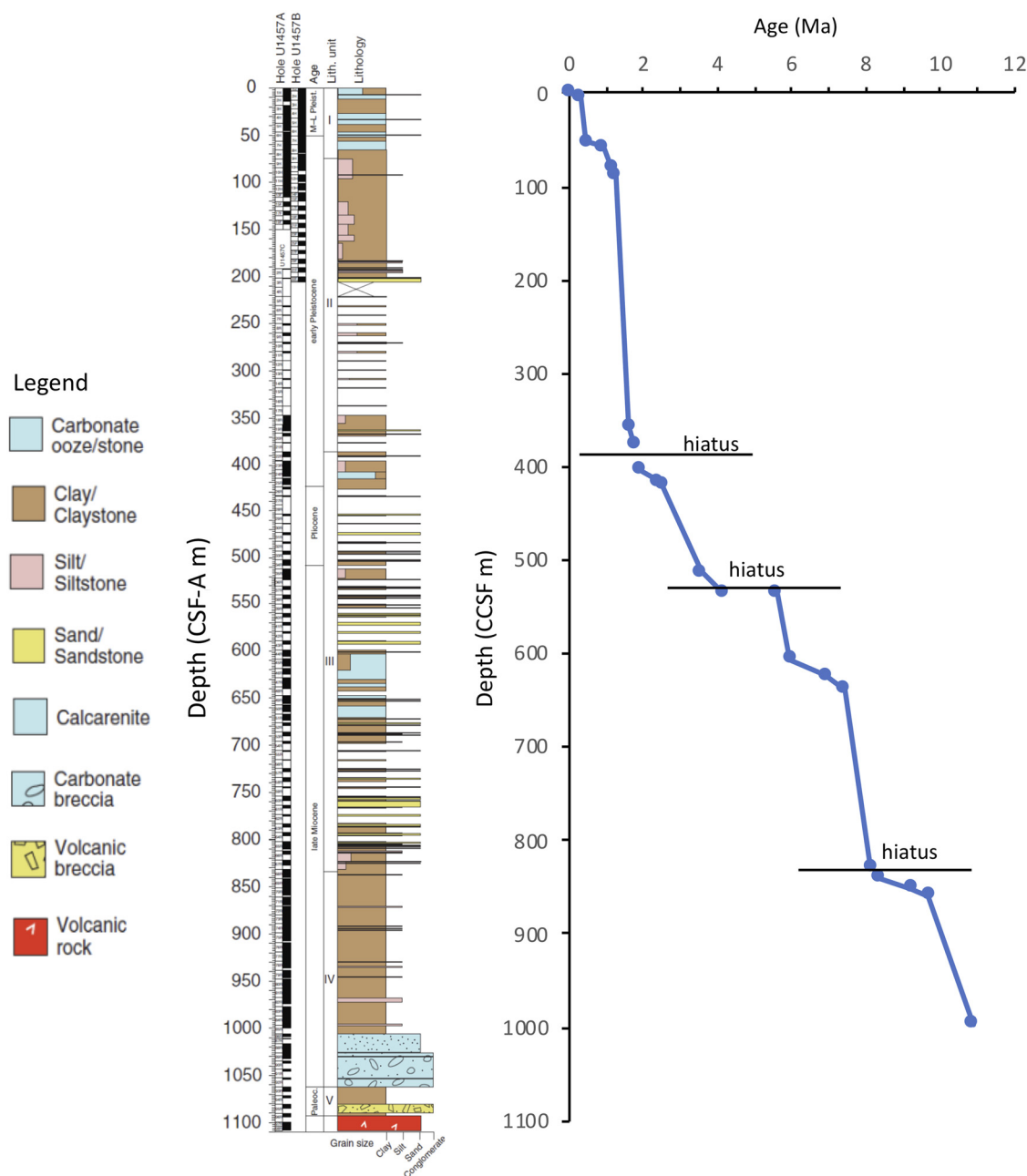
Fig. 2. Lithologic column of Site U1457 and the age–depth model based on biostratigraphic constraints.

(2:1) (neutral fraction) and subsequent 3 ml diethyl ether–acetic acid (96:4) (acid fraction) following Gao *et al.* (2012). The acid fraction dissolved in 0.3 ml toluene was methylated with 1 ml methanol–acetyl chloride (95:5) under nitrogen gas at 60°C for 12 hours. The methylated acid fraction was supplemented with 1 ml 5 % sodium chloride in water and extracted (× 3) with hexane. The fraction was further purified with SiO₂ column chromatography: 3 ml hexane and subsequent 3 ml dichloromethane (methylated acid fraction for analysis).

Gas chromatography (GC) was conducted using an Agilent 6890 series gas chromatograph with on-column injection and electronic pressure control systems, and a flame ionization detector. Samples were dissolved in hexane. Helium was the carrier gas and the flow velocity was maintained at 30 cm s⁻¹. A Chrompack CP-Sil5CB column was used (length, 50 m; i.d., 0.32 mm; thickness,

0.25 µm). The oven temperature was programmed from 50°C to 120°C at 30°C min⁻¹, and from 120°C to 310°C at 5°C/min⁻¹, and then maintained at 310°C for 30 minutes.

The carbon preference index (CPI) and averaged chain length (ACL) of n-fatty acids are defined in this study as:

$$CPI = 0.5\{(C_{26} + C_{28} + C_{30} + C_{32})/(C_{25} + C_{27} + C_{29} + C_{31})$$
$$+ (C_{26} + C_{28} + C_{30} + C_{32})/(C_{27} + C_{29} + C_{31} + C_{33})\}$$
$$ACL = (24C_{24} + 26C_{26} + 28C_{28} + 30C_{30} + 32C_{32})$$
$$/(C_{24} + C_{26} + C_{28} + C_{30} + C_{32})$$

Combined GC-isotope ratio-mass spectrometry (GC/IRMS) for n-fatty acids was carried out using an Agilent 6890 series gas chromatograph with a capillary column coated with DB-5MS

Table 1. Biostratigraphic datums used for the age–depth model of Site U1457 in this study

Datum	Age (Ma)	Depth (mbsf)	Depth (CCSF m)	Reference
LO of *Emiliania huxleyi*	0.29	14.02	18.91	1
FO of *Pseudoemiliania lacunosa*	0.44	45.56	52.42	1
LO of *Reticulofenestra asanoi*	0.91	50.32	56.94	1
FO of *Reticulofenestra asanoi*	1.14	72.08	78.46	1
LO of *Gephyrocapsa* spp. >5.5 μm	1.24	83.78	90.62	1
FO of *Gephyrocapsa* spp. >5.5 μm	1.62	356.60	356.60	1
FO of *Gephyrocapsa* spp. >4 μm	1.73	376.03	376.03	1
LO of *Discoaster brouweri*	1.93	403.83	403.83	1
LO of *Discoaster pentaradiatus*	2.39	415.35	415.35	1
LO of *Discoaster surculus*	2.49	418.82	418.82	2
LO of *Sphenolithus* spp.	3.54	512.30	512.30	2
FO of *Discoaster tamalis*	4.13	534.00	534.00	2
LO of *Discoaster quinqueramus*	5.59	534.53	534.53	1
LO of *Nicklithus amplificus*	5.94	605.21	605.21	2
FO of *Nicklithus amplificus*	6.91	623.19	623.19	2
FO of *Amaurolithus* spp.	7.42	638.42	638.42	2
FO of *Discoaster quinqueramus*	8.12	827.70	827.70	1
LO of *Minylitha convallis*	8.38	840.47	840.47	1
LO of *Discoaster bollii*	9.21	851.35	851.35	1
LO of *Catinaster coalitus*	9.69	859.49	859.49	1
FO of *Catinaster coalitus*	10.89	995.93	995.93	1

1 – Pandey *et al.* (2016); 2 – C. M. Routledge (unpub. M.Sc. thesis, Florida State Univ., 2015).

(30 m length; i.d. 0.32 mm; 0.25 μm film thickness) combined with a Finnigan MAT delta Plus mass spectrometer through a combustion furnace at 850°C. GC conditions were the same as above. As an internal isotopic standard, *n*-$C_{36}H_{74}$ was used to check the condition of measurements. Data were converted to values relative to the Vienna Pee Dee Belemnite (VPDB) using standard delta notation by comparison with CO_2 standard gas.

The $\delta^{13}C$ value of methanol (source of methylated carbon) used in this study was –34.1 ± 0.2 ‰. Hence, the $\delta^{13}C$ value of fatty acids was calculated as:

$$\delta^{13}C_{free} = \{(C_n + 1)\delta^{13}C_{ester} + 34.1\}/C_n$$

where $\delta^{13}C_{free} = \delta^{13}C$ of free acid, $\delta^{13}C_{ester} = \delta^{13}C$ of methyl ester and C_n = carbon number of the free acid. Reproducibility of the measurements based on repeated analyses is better than ±0.5 ‰.

3. Results

3.a. The carbon number distribution of n-fatty acids

Normal fatty acids have a bimodal pattern of carbon number distribution showing maxima at C_{16} and C_{26}/C_{28} and a strong even carbon number preference (Fig. 3; online Supplementary Material Table S1). The CPI ranged from 2.8 to 5.4, which is common in higher plant leaf waxes (e.g. Chikaraishi & Naraoka, 2007). The CPI tended to increase with significant fluctuation from 10.6 to 6 Ma, and to decrease slightly after 3.6 Ma (Fig. 4). The carbon number distribution was characterized by relatively abundant mid-chain C_{24} homologue. The ACL fluctuated on a million-year timescale with maxima around 8, 6, 3–2 and 1.3 Ma (Fig. 4).

3.b. $\delta^{13}C$ values of n-fatty acids

The $\delta^{13}C$ values of long- and mid-chain n-fatty acids followed different trends from 10.8 to 6.3 Ma (Fig. 4; online Supplementary Material Table S1). The $\delta^{13}C$ of long-chain *n*-C_{32} fatty acid shifted from −34 to −22 ‰ from 10.4 to 6.3 Ma, while the $\delta^{13}C$ of mid-chain *n*-C_{24} fatty acid was consistently around −23 to −22 ‰, with the exception of a significant negative excursion around 8 Ma. The $\delta^{13}C$ values of *n*-C_{24} fatty acid were always higher than those of *n*-C_{32} fatty acid before 6.3 Ma. The $\delta^{13}C$ values of *n*-C_{26} to *n*-C_{30} fatty acids were intermediate between those of C_{24} and *n*-C_{32} fatty acids. After 6.3 Ma, the $\delta^{13}C$ values of long- and mid-chain n-fatty acids did not change significantly.

4. Discussion

4.a. Major sources of long- and mid-chain n-fatty acids

The $\delta^{13}C$ of *n*-C_{32} fatty acid shifted from −34 to −22 ‰ from 10.4 to 6.3 Ma (Fig. 4). This positive shift in the $\delta^{13}C$ of n-alkanes was also reported in a previous study of the Arabian Sea and was attributed to an increased abundance of C_4 plants (Huang *et al.* 2007). However, alternate interpretations are possible based on the $\delta^{13}C$ values and concentrations of *n*-C_{24} to *n*-C_{32} fatty acids in the study samples.
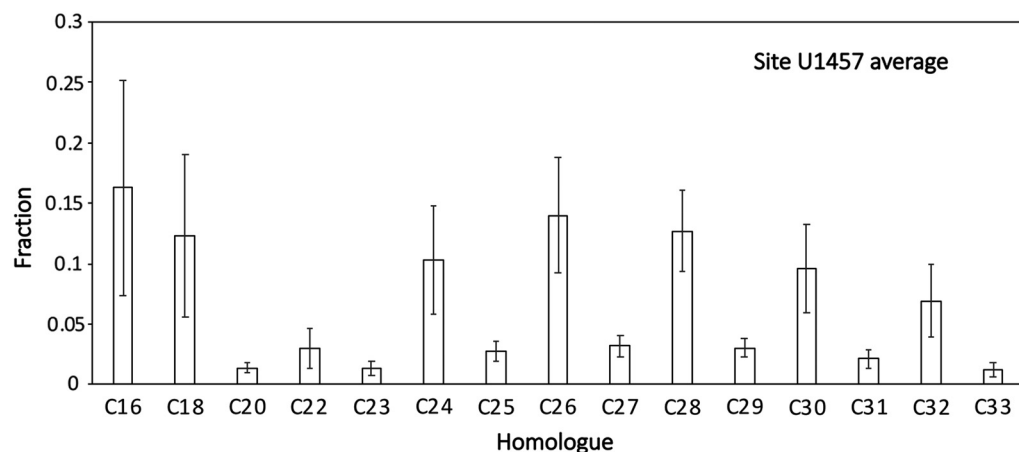
Fig. 3. Averaged carbon number distribution of n-fatty acids at Site U1457.

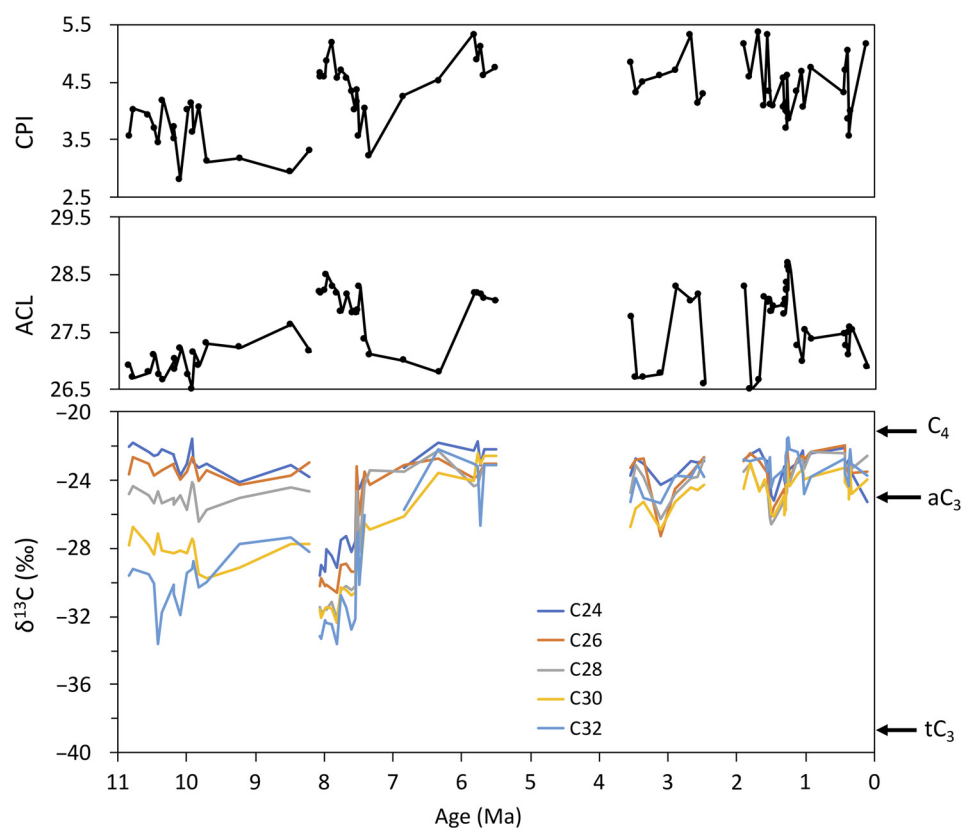**Fig. 4.** Carbon number preference index (CPI), averaged chain length (ACL) of n-fatty acids and the δ¹³C of n-C₂₄ to n-C₃₂ fatty acids in sediments from Site U1457 during the last 10.6 million years. Arrows indicate the average values of terrestrial C₃, aquatic C₃ and C₄ plants (tC₃, aqC₃ and C₄, respectively; Chikaraishi *et al.* 2004).

The δ¹³C values of long- and mid-chain n-fatty acids followed different patterns from 10.8 to 6.3 Ma (Fig. 4). This observation cannot be explained if we assume that C₃ and C₄ terrestrial plants were the sole sources of these n-fatty acids, as C₃ and C₄ terrestrial plants have nearly identical patterns of n-fatty acid distribution, and little difference in the δ¹³C exists among homologues in single species (Chikaraishi *et al.* 2004; Chikaraishi & Naraoka, 2007). Ficken *et al.* (2000) reported that the n-fatty acids of aquatic vascular C₃ plants are characterized by a homologous distribution with a maximum around C₂₄ (ACL = 26.6), whereas terrestrial vascular plants have a maxima around C₃₀ (ACL = 28.6). Chikaraishi *et al.* (2004) reported that the free n-fatty acids (C₃₀ and C₃₂) of aquatic vascular C₃ plants have δ¹³C values of −24.8 ± 1.5 ‰, which is close to the value for C₄ plants (−21.1 ± 1.1 ‰) and higher than that for terrestrial vascular C₃

plants (−38.5 ± 3.4 ‰). Thus, the large difference in the δ¹³C values of mid-chain (C₂₄ and C₂₆) and long-chain (C₃₀ and C₃₂) fatty acids from 10.8 to 6.3 Ma may be attributable to the contribution of aquatic C₃ plants such as freshwater submerged and floating plants and sea grasses.

The plot of the ACL and the δ¹³C values of long-chain fatty acids demonstrates that most U1457 samples group within a triangle of C₃ angiosperm trees, C₄ plants and aquatic C₃ plants (Fig. 5). Before 6.3 Ma, the ACL and the δ¹³C values of long-chain fatty acids were negatively correlated (Fig. 5), suggesting that the δ¹³C values reflected the relative contribution of terrestrial C₃ versus aquatic C₃ plants in the Indus River basin and western India. The samples of 10.8–8.3 Ma are distributed along the line between terrestrial and aquatic C₃ plant end-members, implying a negligible contribution of C₄ plants. The samples of 8.1–7.5 Ma are distributed
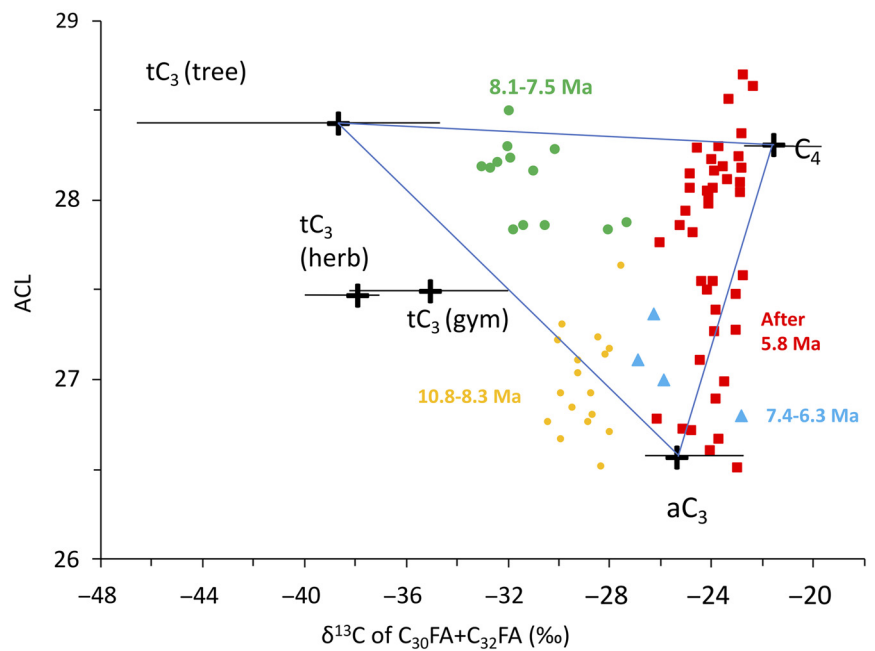
Fig. 5. Plots of the average chain length (ACL) against the $\delta^{13}C$ of n-C_{30} and n-C_{32} fatty acids in Site U1457 samples. Yellow circles, green circles, blue triangles and red squares indicate samples from 10.8–8.3 Ma, 8.1–7.5 Ma, 7.4–6.3 Ma and 5.8–0 Ma, respectively. The diagram shows the $\delta^{13}C$ ranges (horizontal bars) and average of literature values of terrestrial and aquatic C_3 plants (tC_3 and aC_3) and C_4 plants (C_4).
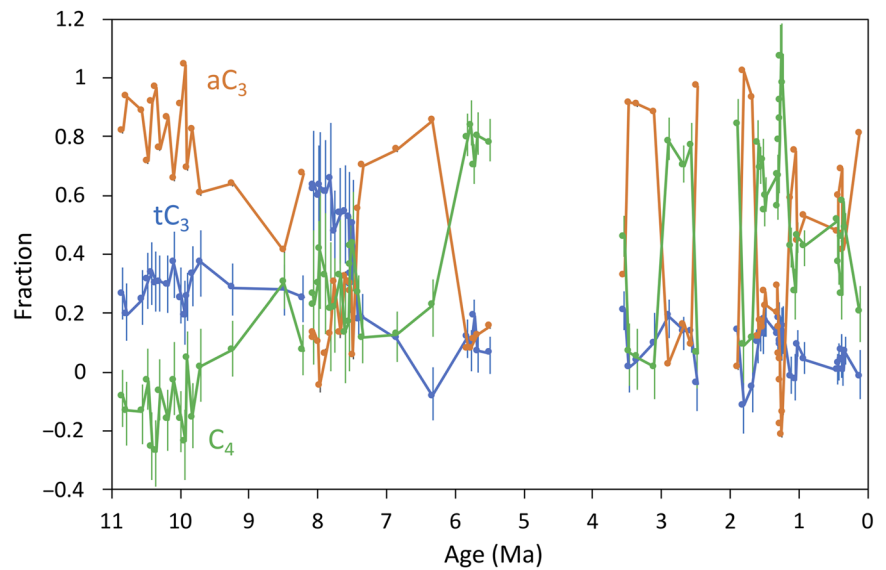

Fig. 6. The relative abundance of terrestrial and aquatic C_3 plants (tC_3 and aC_3) and C_4 plants in U1457 sediments during the last 10.6 million years. Vertical bars indicate the range of fractions calculated from the minimum and maximum $\delta^{13}C$ end-member values.

near the line between terrestrial C_3 and C_4 plant end-members, indicating a significant contribution of terrestrial plants including C_4 plants. After 5.8 Ma, the $\delta^{13}C$ values remained constant and were independent of the ACL (Fig. 5), suggesting that the $\delta^{13}C$ values reflected heavier $\delta^{13}C$ values of both aquatic C_3 and C_4 plants. The relative contribution of terrestrial C_3 (f_{tC3}), aquatic C_3 plants (f_{aC3}) and C_4 plants (f_{C4}) was estimated from the end-members of their ACL and C_{30} and C_{32} $\delta^{13}C$ values following the equations:

$$f_{tC3} + f_{aC3} + f_{C4} = 1$$

$$\delta^{13}C_{tC3}f_{tC3} + \delta^{13}C_{aC3}f_{aC3} + \delta^{13}C_{C4}f_{C4} = \delta^{13}C$$

$$ACL_{tC3}f_{tC3} + ACL_{aC3}f_{aC3} + ACL_{C4}f_{C4} = ACL$$

where $\delta^{13}C_{tC3} = -38.5$ ‰ (−46.8 to −34.5 ‰, n = 10, Chikaraishi & Naraoka, 2007), $\delta^{13}C_{aC3} = -24.8$ ‰ (−26.5 to

−22.8 ‰, n = 3, Chikaraishi *et al.* 2004), $\delta^{13}C_{C4} = -21.1$ ‰ (−22.6 to −19.7 ‰, n = 5, Chikaraishi & Naraoka, 2007), $ACL_{tC3} = 28.5$ (Chikaraishi & Naraoka, 2007), $ACL_{aC3} = 26.6$ (Ficken *et al.* 2000) and $ACL_{C4} = 28.3$ ACL (Chikaraishi & Naraoka, 2007) as the end-members. The datasets of $\delta^{13}C$ and ACL of end-members are not comprehensive and contain uncertainty. To estimate the influence of end-member $\delta^{13}C$ values, the fractions f_{tC3}, f_{aC3} and f_{C4} were calculated from the average, minimum and maximum $\delta^{13}C$ end-member values. The end-member $\delta^{13}C$ value of each plant component changed from the minimum to maximum, and the fractions f_{tC3}, f_{aC3} and f_{C4} were calculated for each case (Fig. 6). We chose the values of C_3 angiosperm trees rather than C_3 angiosperm herbs and gymnosperms as a representative of terrestrial C_3 plants because the values derived from C_3 angiosperm trees can better explain the variations of the ACL and $\delta^{13}C$ prior to 6.3 Ma (Fig. 5). The
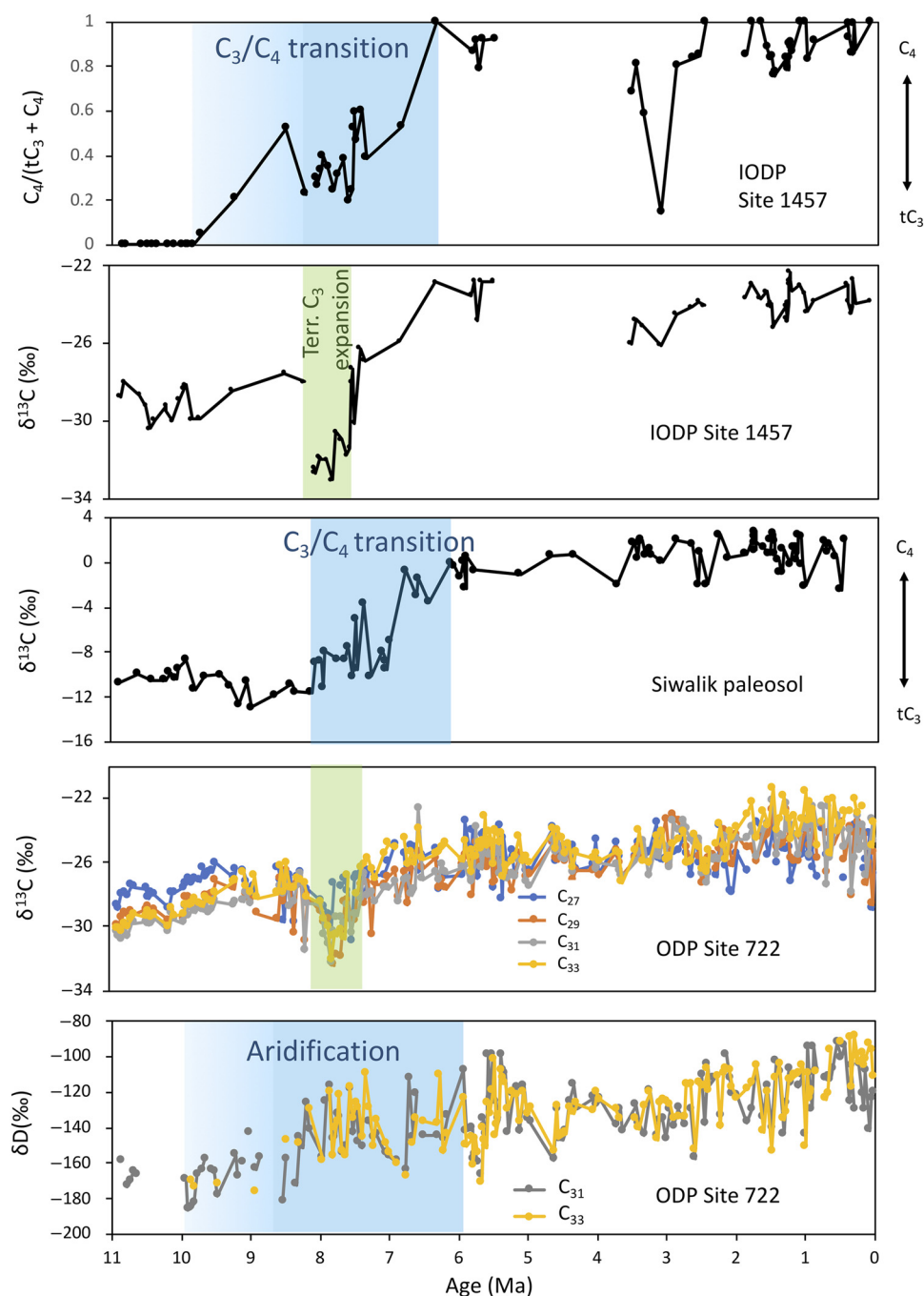
Fig. 7. The relative abundance of C$_4$ plants in terrestrial plants (C$_4$/(tC$_3$ + C$_4$)) and the δ^{13}C of n-C$_{30}$ and n-C$_{32}$ fatty acids at Site U1457 (this study); the δ^{13}C of soil carbonate in the Siwalik palaeosol in Pakistan (Huang *et al*. 2007); and the δ^{13}C of n-C$_{27}$, n-C$_{29}$, n-C$_{31}$ and n-C$_{33}$ alkanes and the δD of n-C$_{31}$ and n-C$_{33}$ alkanes at Site 722 in the Arabian Sea (Huang *et al*. 2007) during the last 10.6 million years.

end-member calculation indicates drastic changes in the relative abundances of terrestrial C$_3$ (f$_{tC3}$), aquatic C$_3$ plants (f$_{aC3}$) and C$_4$ plants (f$_{C4}$) during the last 10.8 Myr. Aquatic C$_3$ plants were generally abundant most of the time, but terrestrial C$_3$ plants dominated from 8.1 to 7.5 Ma, and C$_4$ plants dominated intermittently after 6 Ma (Fig. 6).

In contrast to our findings, no significant variation in different homologues has been observed at Site 722 in the δ^{13}C of C$_{27}$–C$_{33}$ n-alkanes from 10.6 to 6 Ma. All of homologues show similar values (Fig. 7; Huang *et al*. 2007). This suggests either a lesser influence of the contribution of aquatic plants to the δ^{13}C of long-chain n-alkanes or a minimal contribution from aquatic C$_3$ plants to the

Site 722 sediments. The n-alkanes in aquatic plants are typically dominated by mid-chain homologues than are n-fatty acids (Ficken *et al*. 2000). The difference in the homologous distribution may have led to the lesser influence of the contribution of aquatic plants to the δ^{13}C of long-chain n-alkanes, even with a significant contribution of aquatic C$_3$ plants. Alternatively, Site 722 is located on Owen Ridge and is therefore unaffected by turbidite deposition on the adjacent Indus Fan. Aeolian transport is the principal pathway for terrestrial input to the site (Clemens *et al*. 1996). Because of this depositional setting, the leaf wax record of Site 722 does not reflect the contribution of aquatic plants in the Indus and western Indian river waters.
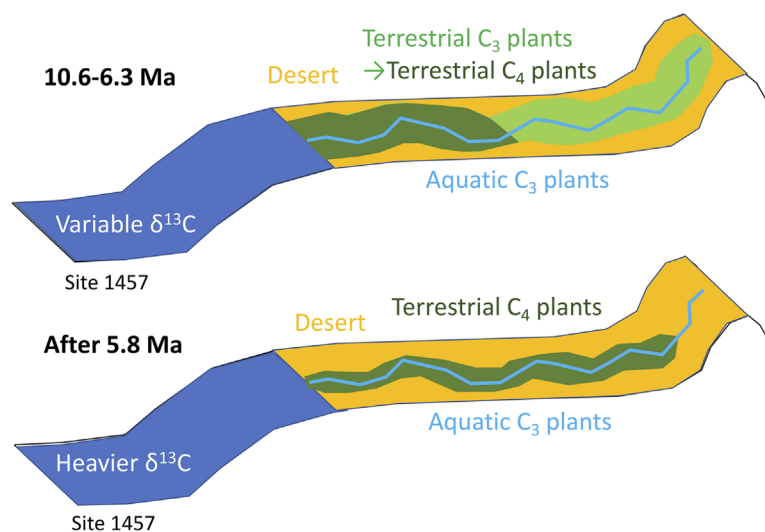
Fig. 8. Schematic views of vegetation in the Indus and western Indian river basins before and after 6.3 Ma.

4.b. Late Miocene vegetation changes in the Indus River basin and western India

The abundance of C_4 plants in total terrestrial C_3 and C_4 plants, i.e. the $C_4/(tC_3 + C_4)$ ratio, suggests that the terrestrial C_3 plants were replaced by C_4 plants in the Indus River basin and western India from 9.7 to 6.3 Ma with a period of terrestrial C_3 plant expansion around 8 Ma (Fig. 7). However, whether the onset of C_4 plant expansion occurred at 9.7 Ma or 8.2 Ma is not clear because the contribution of aquatic C_3 plants overprinted the $\delta^{13}C$ signal of C_4 plants. The high $C_4/(tC_3 + C_4)$ ratio at 8.5 Ma is a single peak, and the ratios of other samples from 9.7–8.2 Ma are not significantly higher than 0 (Fig. 7). The robust increase in the $C_4/(tC_3 + C_4)$ ratio started at 8.2 Ma, which was synchronous with the increase in the $\delta^{13}C$ value of palaeosol carbonate in Siwalik palaeosol sequences (Fig. 7; Huang *et al.* 2007; Behrensmeyer *et al.* 2007), although the $\delta^{13}C$ value of palaeosol carbonate (Sanyal *et al.* 2004; Behrensmeyer *et al.* 2007) and long-chain n-alkanes (Ghosh *et al.* 2017) in Siwalik palaeosol sequences showed various changing patterns due to differences in the sub-environments of the Siwalik alluvial plain (Behrensmeyer *et al.* 2007). This trend is consistent with the occurrence of aridification in the Indus River basin and western India, which was indicated by positive shifts in the $\delta^{18}O$ of soil carbonate in Siwalik palaeosols (Quade *et al.* 1989; Quade & Cerling, 1995; Sanyal *et al.* 2004; Behrensmeyer *et al.* 2007; Huang *et al.* 2007) and the δD of long-chain n-alkanes at ODP Site 722 in the Arabian Sea (Fig. 7; Huang *et al.* 2007). A modelling study with the boundary conditions of the late Miocene palaeogeography, orography and ice sheets and an atmospheric CO_2 level of 395 ppm indicated that the Indus River basin and western India were covered by tropical forests and shrubs in the Tortonian Age (11.6–7.3 Ma) because precipitation levels were 1−2 mm/day higher than at present (Pound *et al.* 2011). An isotope study for river waters in the Indus River basin indicated that 64 to 72 % of the Indus waters are derived from moisture transport from the Mediterranean Sea, and the rest derives from the Indian summer monsoon at present (Karim & Veizer, 2002). Intensification of the Indian summer monsoon after 8 Ma, shown in marine foraminifera records (e.g. Kroon *et al.* 1991; Prell *et al.* 1992), is not consistent with the expansion of a C_4 ecosystem in the Indus River basin. Instead, during the Messinian Age (7.3–5.3 Ma), the shrinkage

of the Paratethys and Mediterranean seas (Ivanov *et al.* 2011) may have decreased moisture transport to the Indus River basin and western India. Decreased precipitation in the Indus River basin and western India during late Miocene time may have driven the replacement of terrestrial C_3 plants by C_4 plants in this region.

If the increase of the $C_4/(tC_3 + C_4)$ ratio from 9.7 Ma is real, the replacement of C_3 plants by C_4 plants in the Indus River basin and western India began before the positive shift in the $\delta^{13}C$ value of palaeosol carbonate in Siwalik palaeosol sequences in the northern Indus River basin (Fig. 7; Quade *et al.* 1989; Quade & Cerling, 1995; Huang *et al.* 2007). One possible interpretation is that C_3/C_4 replacement started earlier in the downstream area of the Indus River and western India than in the upstream area of the Indus River (Fig. 8). Higher levels of precipitation in the Himalaya Mountains may have supplied sufficient water to C_3 vegetation in the upstream area. This interpretation is consistent with the distribution of modern and Holocene vegetation in the Indus River basin (Ivory & Lézine, 2009).

An episodic negative excursion of the $\delta^{13}C$ values of n-C_{30} and n-C_{32} fatty acids around 8 Ma was superimposed on an increasing trend of $\delta^{13}C$ (Fig. 7). Because it is associated with the increase in terrestrial C_3 plants and the decrease in aquatic C_3 plants (Fig. 6), this excursion suggests that the contribution of terrestrial C_3 plants was elevated compared with that of aquatic C_3 plants in the Indus and western Indian river waters. A pollen study of Holocene sediments from core SO90-56KA recovered from the Makran coast (Indus margin) of the Arabian Sea indicates more abundant montane pollen taxa from the Himalayas when the Indian summer monsoon was stronger due to increased fluvial activity of the Indus River during those times (Ivory & Lézine, 2009). In contrast, pollen taxa from shrubs in the lower reaches of the Indus River were relatively abundant when the Indian summer monsoon was weaker. This observation suggests that higher precipitation in the upper reaches of the Indus River may have increased the contribution of terrestrial C_3 plants in the Indus Fan sediments.

The negative excursion at 8 Ma was also recorded at ODP Site 722 in the Arabian Sea (Fig. 7; Huang *et al.* 2007). Site 722 received terrestrial sediments transported from Pakistan, Iran, Afghanistan and the Arabian Peninsula by wind, suggesting that the excursion

was a regional, rather than local, phenomenon (Clemens *et al.* 1996; Huang *et al.* 2007). The negative excursion around 8 Ma can be correlated with the second 'washhouse' event of elevated precipitation in Europe (Böhme *et al.* 2008). Enhanced moisture transport from Europe to the Indus River basin increased precipitation. Increased precipitation may have allowed range expansion for terrestrial grassland and forest, increasing the proportion of terrestrial C_3 plants to aquatic plants in the Indus River and causing the negative $\delta^{13}C$ excursion.

5. Conclusions

A large difference in the $\delta^{13}C$ values of mid-chain (C_{24} and C_{26}) and long-chain (C_{30} and C_{32}) fatty acids from 10.6 Ma to 6.3 Ma suggests the contribution of aquatic C_3 plants. Before 6.3 Ma, the $\delta^{13}C$ values reflected the relative abundance of terrestrial C_3 versus aquatic C_3 and C_4 plants in the Indus River basin and western India. After 6.3 Ma, the $\delta^{13}C$ values reflected heavier $\delta^{13}C$ values of both C_3 aquatic and C_4 plants.

A three-end-member model calculation suggests that terrestrial C_3 plants were replaced by C_4 plants in the Indus River basin and western India from 9.7 or 8.2 to 6.3 Ma. Decreased precipitation in those areas during late Miocene time may have driven the replacement of terrestrial C_3 plants by C_4 plants. The shrinkage of the Paratethys and Mediterranean seas (Ivanov *et al.* 2011) may have decreased moisture transport to the Indus River basin and western India.

An episodic increase in terrestrial C_3 and C_4 plants around 8 Ma was superimposed on a decreasing trend of terrestrial C_3 plants. The increase can be attributed to high precipitation caused by the regionally enhanced moisture transport from the west.

References

Behrensmeyer AK, Quade J, Cerling TE, Kappelman J, Khan IA, Copeland P, Roe L, Hicks J, Stubblefield P, Willis BJ and Latorre C (2007) The structure and rate of late Miocene expansion of C_4 plants: evidence from lateral variation in stable isotopes in paleosols of the Siwalik Group, northern Pakistan. *Geological Society of America Bulletin* **119**, 1486–505.

Böhme M, ILG A and Winkhofer M (2008) Late Miocene "washhouse" climate in Europe. *Earth and Planetary Science Letters* **275**, 393–401.

Cerling TE, Ehleinger JR and Harris JM (1998) Carbon dioxide starvation, the development of C4 ecosystems, and mammalian evolution. *Philosophical Transactions of the Royal Society of London B* **353**, 159−71.

Chikaraishi Y and Naraoka H (2007) δ¹³C and δD relationships among three n-alkyl compound classes (n-alkanoic acid, n-alkane and n-alkanol) of terrestrial higher plants. *Organic Geochemistry* **38**, 198−215.

Chikaraishi Y, Naraoka H and Poulson SR (2004) Hydrogen and carbon isotopic fractionations of lipid biosynthesis among terrestrial (C3, C4 and CAM) and aquatic plants. *Phytochemistry* **65**, 1369−81.

Clemens SC, Murray DW and Prell WL (1996) Nonstationary phase of the Plio-Pleistocene Asian Monsoon. *Science* **274**, 943−8.

Clift PD, Campbell IH, Pringle MS, Carter A, Zhang X, Hodges KV, Khan AA and Allen CM (2004) Thermochronology of the modern Indus River bedload; new insight into the controls on the marine stratigraphic record. *Tectonics* **23**, TC5013. doi: 10.1029/2003TC001559.

Clift PD, Zhou P, Stockli DF and Blusztajn J (2019) Regional Pliocene exhumation of the Lesser Himalaya in the Indus drainage. *Solid Earth* **10**, 647−61. doi: 10.5194/se-10-647-2019.

Edwards EJ, Obsorne CP, Stromberg CAE, Smith SA and C4 Grasses Consortium (2010) The origins of C_4 grasslands: integrating evolutionary and ecosystem science. *Science* **328**, 587−91.

Ficken KJ, Li B, Swan DL and Eglington G (2000) An n-alkane proxy for the sedimentary input of submerged/floating freshwater aquatic macrophytes. *Organic Geochemistry* **31**, 745−9.

Galy V, Francois L, France-Lanord C, Faure P, Kudrass H, Palhol F and Singh SK (2008) C_4 plants decline in the Himalayan basin since the Last Glacial Maximum. *Quaternary Science Reviews* **27**, 1396–409.

Gao L, Burnier A and Huang Y (2012) Quantifying instantaneous regeneration rates of plant leaf waxes. *Rapid Communications in Mass Spectrometry* **26**, 115–22.

Garzanti E, Vezzoli G, Ando S, Paparella P and Clift PD (2005) Petrology of Indus River sands: a key to interpret erosion history of the Western Himalayan syntaxis. *Earth and Planetary Science Letters* **229**, 287–302.

Ghosh S, Sanyal P and Kumar R (2017) Evolution of C4 plants and controlling factors: insight from n-alkane isotopic values of NW Indian Siwalik paleosols. *Organic Geochemistry* **110**, 110–21.

Herbert TD, Lawrence KT, Tzanova A, Peterson LC, Caballero-Gill R and Kelly CS (2016) Late Miocene global cooling and the rise of modern ecosystems. *Nature Geoscience* **9**, 843−7.

Huang Y, Clemens SC, Liu W, Wang L and Prell WL (2007) Large-scale hydrological change drove the late Miocene C_4 plant expansion in the Himalayan foreland and Arabian Peninsula. *Geology* **35**, 531−4.

Ivanov D, Utescher T, Mosbrugger V, Syabryaj S, Djorjevic-Milutinovic D and Molchanoff S (2011) Miocene vegetation and climate dynamic in Eastern and Central Paratethys (Southern Europe). *Palaeogeography, Palaeoclimatology, Palaeoecology* **304**, 262−75.

Ivory SJ and Lézine AM (2009) Climate and environmental change at the end of the Holocene Humid Period: a pollen record off Pakistan. *Comptes Rendus Geoscience* **341**, 760−9.

Karim A and Veizer J (2002) Water balance of the Indus River Basin and moisture source in the Karakoram and western Himalayas: implication from hydrogen and oxygen isotopes in river water. *Journal of Geophysical Research* **107**, 4362. doi: 10.1029/2000JD000253.

Kroon D, Steen T and Troelstra SR (1991) Onset of monsoonal related upwelling in the western Arabian Sea as revealed by planktonic foraminifers. *Proceedings of the Ocean Drilling Program, Scientific Results, vol. 117* (eds WL Prell, N Niitsuma, K-C Emeis, ZK Al-Sulaiman, ANK Al-Tobbah, DM Anderson, RO Barnes, RA Bilak, J Bloemendal, CJ Bray, WH Busch, SC Clemens, P de Menocal, P Debrabant, A Hayashida, JOR Hermelin, RD Jarrard, LA Krissek, D Kroon, DW Murray, CA Nigrini, TF Pedersen, W Ricken, GB Shimmield, SA Spaulding, T Takayama, HL ten Haven and GP Weedon), pp. 257−63. College Station, Texas.

Pagani M, Freeman KH and Arthur MA (1999) Late Miocene atmospheric CO_2 concentrations and the expansion of C_4 grasses. *Science* **283**, 876−9.

Pandey DK, Clift PD, Kulhanek DK and The Expedition 355 Scientists (2016) *Proceedings of the International Ocean Discovery Program, vol. 355*. College Station, Texas.

Polissar PJ, Rose C, Uno KT, Phelps SR and Demenocal P (2019) Synchronous rise of African C$_4$ ecosystems 10 million years ago in the absence of aridification. *Nature Geoscience* **12**, 657−60.

Pound MJ, Haywood AM, Salzmann U, Riding JB, Lunt DJ and Hunter SJ (2011) A Tortonian (Late Miocene, 11.61−7.25 Ma) global vegetation reconstruction. *Palaeogeography, Palaeoclimatology, Palaeoecology* **300**, 29−45.

Prell WL, Murray DW, Clemens SC and Anderson DM (1992) Evolution and variability of the Indian Ocean Summer Monsoon: evidence from the western Arabian Sea drilling program. In *Synthesis of Results from Scientific Drilling in the Indian Ocean* (eds RA Duncan, DK Rea, RB Kidd, U von Rad and JK Weissel), pp. 447−69. American Geophysical Union Monograph vol. 70. Washington, DC, USA.

Quade J and Cerling TE (1995) Expansion of C$_4$ grasses in the Late Miocene of Northern Pakistan: evidence from stable isotopes in paleosols. *Palaeogeography, Palaeoclimatology, Palaeoecology* **115**, 91−116.

Quade J, Cerling TE and Bowman JR (1989) Development of Asian monsoon revealed by marked ecological shift during the latest Miocene in northern Pakistan. *Nature* **342**, 163−6.

Sage RF (2004) The evolution of C$_4$ photosynthesis. *New Phytologist* **161**, 342−70.

Sanyal P, Bhattacharya SK, Kumar R, Ghosh SK, and Sangode SJ (2004) Mio-Pliocene monsoonal record from Himalayan foreland basin (Indian Siwalik) and its relation to vegetational change. *Palaeogeography, Palaeoclimatology, Palaeoecology* **205**, 23−41.

Sosdian SM, Greenop R, Hain MP, Foster GL, Pearson PN and Lear CH (2018) Constraining the evolution of Neogene ocean carbonate chemistry using the boron isotope pH proxy. *Earth and Planetary Science Letters* **498**, 362−76.

Still CJ, Berry JA, Collatz GJ and DeFries RS (2003) Global distribution of C$_3$ and C$_4$ vegetation: carbon cycle implications. *Global Biogeochemical Cycles* **17**, 1006. doi: 10.1029/2001GB001807.

Tipple BJ and Pagani M (2007) The early origins of terrestrial C$_4$ photosynthesis. *Annual Review of Earth and Planetary Sciences* **35**, 435−61.

Yu Z, Colin C, Wan S, Saraswat R, Song L, Xu Z, Clift P, Lu H, Lyle M, Kulhanek D, Hahn A, Tiwari M, Mishra R, Miska S, Kumar A (2019) Sea level-controlled sediment transport to the eastern Arabian Sea over the past 600 kyr: clay minerals and Sr–Nd isotopic evidence from IODP site U1457. *Quaternary Science Reviews* **205**, 22–34.